ACS Macro Letters

Letter

pubs.acs.org/macroletters

Patterning by Photochemically Directing the Marangoni Effect

Joshua M. Katzenstein, Dustin W. Janes, Julia D. Cushen, Nikhil B. Hira, Dana L. McGuffin, Nathan A. Prisco, and Christopher J. Ellison*

Department of Chemical Engineering, The University of Texas at Austin, Austin, Texas 78712, United States

Supporting Information

ABSTRACT: Polystyrene (PS) that has been exposed to ultraviolet light (UV) undergoes partial dehydrogenation of the alkane polymer backbone which increases its surface energy. Exploiting this photochemistry, we exposed polystyrene films to UV light using a photomask to induce a patterned photochemical reaction producing regions in the film with differing surface energy. Upon heating the solid polymer film with the preprogrammed surface energy pattern to a liquid state, the polymer flows from the low surface energy unexposed regions to high surface energy exposed regions. This flow creates three-dimensional topography by the Marangoni Effect, which describes convective mass transfer due to surface energy gradients. The topographical features can be permanently preserved by quenching the film below its glass to liquid transition temperature. Their shape and organization are only limited by the pattern on the photomask.

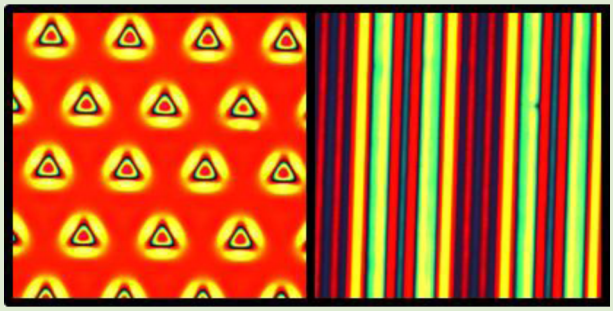

Small variations in temperature or composition at a fluid interface, often spontaneously generated, can cause local changes in surface energy and promote dramatic movement of fluids. This phenomenon, referred to as the Marangoni Effect,[1,2] is familiar to most people in the "tears" or "legs" that form in a glass of wine. The effect more generally describes many other phenomena, from thickening of a tear film lipid layer in the human eye[3] to "fingering instabilities" in spreading thin films.[4] It has also been exploited to manipulate the motion and position of fluids,[5,6] to influence the surface roughness of spin-coated films,[7] to align nanoparticles,[8] or to create colloidal crystal films.[9]

Here we describe a new procedure in which surface energy patterns are created in an amorphous, solid polymer film by triggering a photochemical reaction in exposed areas using ultraviolet (UV) light and a photomask. Upon heating the polymer above its glass to liquid transition temperature (T_g), the patterned surface energy directs Marangoni flow of the liquid polymer film to produce a diversity of prescribed topographic structures. These structures are potentially suitable for a variety of applications, such as the facile creation of soft lithography stamps[10] like those used for transistor arrays,[11] microfluidic devices,[12] printing of microparticles,[13] fabrication of templates for guidance of neurite growth,[14] or engineered antifouling surfaces.[15,16] Given the short light exposure time, as little as 10 s is sufficient to induce feature formation, therefore this approach could be compatible with high-speed roll-to-roll processes for patterning large areas.

The formation of surface topography on a polymer film by Marangoni-driven flow consists of two basic steps (Figure 1). First, a polymer film, here polystyrene (PS), is exposed to light, in this case a 200 W metal-halide lamp with broadband output from ~200−600 nm, through a photomask for a short period of time to induce a photochemical reaction in the exposed polymer throughout the depth of the film supported on a silicon wafer or glass slide. Next, the film is heated for 10 min to well above the polymer's T_g (~ 61 °C for this PS) to reduce its viscosity and facilitate flow. During this time, the surface energy pattern imposed by the photochemical reaction induces flow of material from unexposed regions with relatively low surface energy to exposed regions with relatively high surface energy. The result is a prescribed surface topography formed by the Marangoni Effect that was directed by patterning the photochemical reaction during light exposure through the photomask.

The exposure of PS to UV light is known to cause dehydrogenation of the carbon−carbon bonds in the backbone of the polymer chain resulting in double bond formation (Figure 2a).[17−21]These double bonds create "stilbene-like" chemical structures from a portion of the repeat units which have significantly red-shifted fluorescence spectra relative to neat PS. Accordingly, solution fluorimetery was used to qualitatively confirm the creation of stilbene-like structures as evidenced by a significant fluorescence signal at wavelengths where PS precursors do not fluoresce (Figure 2b).[19] PS in tetrahydrofuran (THF) solution samples were prepared for this study for exposed and unexposed films because solid-state PS fluorescence emission is dominated by excited-state phenyl ring dimers which fluoresce in the same region as stilbene-like structures.[22] Furthermore, Marangoni-driven flow does not

Received: August 4, 2012
Accepted: September 4, 2012
Published: September 10, 2012

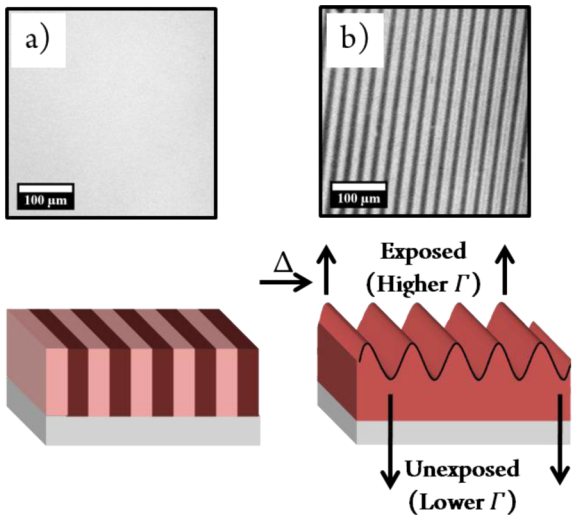

Figure 1. Schematic illustration of the steps involved in feature formation in a PS thin film. (a) A bright-field micrograph of a glassy polymer film (~150 nm thick) after exposure to light through a photomask which induces a photochemical reaction in exposed regions and an associated patterned surface energy. For the PS films employed here, there is higher surface energy in the exposed regions. No topography can be detected by atomic force microscopy after this stage. (b) After heating the same film to 110 °C, where the polymer becomes a liquid, the patterned surface energy drives formation of topographic features via the Marangoni Effect.

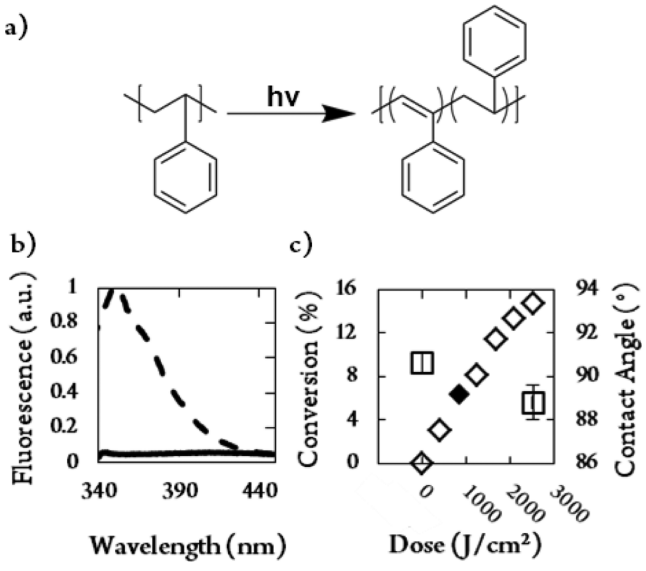

Figure 2. (a) Dehydrogenation reaction of PS by exposure to UV light. (b) Fluorescence spectra of PS precursor (solid line) and PS exposed to UV light for two minutes (dashed line), both in THF solutions at 0.05 mg/mL. For both samples λ_{ex} = 310 nm. (c) Percent conversion of PS backbone to carbon−carbon double bonds as a function of exposure dose by infrared spectroscopy (diamonds). The filled data point represents the typical dose and conversion used in this study. Squares represent the water contact angle of the PS filim as a function of exposure dose. Error bars represent one standard deviation, and the difference between the exposed and unexposed films is statistically significant (t test p-value <0.001).

occur when the UV light absorbed by PS is filtered out from the broadband light source using a long pass filter, even though the overall light intensity is not attenuated significantly (see Supporting Information, Figure 1). This indicates that UV photochemistry of PS is responsible for the surface energy pattern that leads to Marangoni flow and topographic pattern formation.

To more quantitatively assess the extent of the photochemical reaction, Fourier transform infrared spectroscopy (FTIR) (see Supporting Information, Figure 2, for full spectra) was used to follow the dehydrogenation of the PS backbone. As the alkane bonds in the backbone are converted to alkenes, the area under the peak from 2800 to 2964 cm^{-1} corresponding to methylene C−H bond stretching[23] decreases. The dehydrogenation of the PS backbone can be quantified by expressing the decrease in area of this peak relative to that of one unaffected by UV exposure. We used the area under the peak corresponding to the carbonyl (1720 cm^{-1}) of the polymer initiator fragment, a constant, as the normalization factor. Figure 2c shows the percent conversion of the PS backbone to its dehydrogenated form at different UV light exposure doses. From this analysis, the exposure dose used in this study (840 J/cm^2, the total dose from all wavelengths of the broadband source) converts 6.4% of backbone bonds to alkenes. The photoconversion increases monotonically with exposure dose. Additionally, the PS films used in this study (~150 nm thick) absorb <15% of the incident light at the peak absorbance wavelength (260 nm) and <10% of the total broadband incident light. This indicates that the photochemical changes to the polymer should be relatively uniform throughout the depth of the film. Under typical exposure conditions, no surface oxidation was detectable by X-ray photoelectron spectroscopy (see Supporting Information, Figure 3). Molecular weight (M) distribution shifts indicative of cross-linking or scission reactions were not observed by gel permeation chromatography (see Supporting Information, Figure 4) for these conditions. Furthermore, additional experiments were performed to ensure that the mask was not leaving indentations in the polymer film (see Supporting Information, Figure 5). Therefore, we attribute changes in surface energy arising from photoexposure solely to photochemical dehydrogenation of the PS backbone and that Marangoni flow is the mechanism for topography formation.

For topography to form via the Marangoni Effect, the photochemistry must result in exposed regions with sufficiently different surface energy compared to the original PS polymer. Generally, polymers with pure alkane backbones have lower surface energies than analogous polymers with alkene bonds in their backbones. In the simplest examples, poly(butadiene), a polymer with an alkene-containing backbone, and poly(acetylene), consisting of a completely conjugated alkene backbone, have higher surface energies than polyethylene, which has a backbone made up of only alkane bonds.[24] By using a photomask, the conversion of PS to a partially dehydrogenated form by UV photochemistry occurs only within exposed regions of the film, creating a pattern of relatively high (exposed) and low (unexposed) surface energy regions in an originally homogeneous film.

The change in surface chemistry is qualitatively detectable by measuring a test liquid contact angle on the PS film surface. Figure 2c shows a reduction in water contact angle with exposure dose indicative of a change in the chemical structure of the polymer at the surface. Two additional test liquids were evaluated [glycerol and 300 g/mol poly(ethylene glycol)], and all showed a decrease in contact angle following exposure of the PS film to UV light (Supporting Information, Figure 6). It is important to note that determination of the surface energy directly is very challenging for polymers due to their tendency

dx.doi.org/10.1021/mz300400p | ACS Macro Lett. 2012, 1, 1150−1154

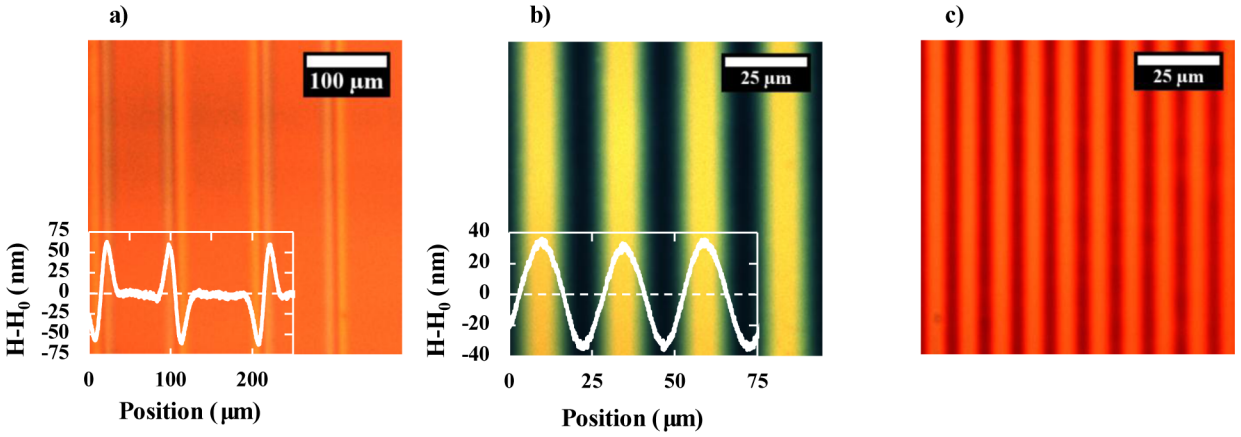

Figure 3. Various line pattern periods created in ~150 nm thick PS films with overlaid profilometry traces showing topography formed by using photomasks with different line spacing of (a) 100 μm chrome lines with a 200 μm pitch, (b) 12.5 μm chrome lines on a 25 μm pitch, and (c) 5 μm chrome lines on a 10 μm pitch. For part (c), the profilometer stylus is too large for accurate characterization of the topography. Panel (a) highlights that Marangoni-driven patterning is sensitive to the local gradient in surface energy, which occurs only near interfaces of exposed and unexposed regions which are a smaller portion of the overall image in (a) than (b) or (c).

to absorb or dissolve in many small molecule test liquids. A simple extrapolation to ~14% conversion between PS and an analog with a dehydrogenated backbone, poly(phenyl acetylene), indicates that the change in test liquid contact angle in Figure 2c corresponds to a change in surface energy of <1 dyn/cm. The Maragoni analysis described in the following paragraph shows that the minimum critical surface energy differences necessary to induce Marangoni driven flow are roughly 0.01 dyn/cm.

To overcome the viscous forces that retard flow, a minimum critical gradient in surface energy is necessary. This value is characterized by the dimensionless Marangoni number[25] defined in eq 1.

$$\mathrm{Ma} = -\frac{\Gamma' H^2 \nabla C_{PS}}{\mu D} \quad (1)$$

In this equation, Ma is the Marangoni number; Γ' is the surface energy change with composition; ∇C_{PS} is the gradient in concentration of PS in the plane of the film; H is the characteristic length of the surface energy gradient, in this case the half pitch of the photomask being used; μ is the viscosity; and D is the diffusion coefficient. Previous research has shown that the critical Marangoni number for instabilities, and therefore for Marangoni flow to occur, is 80.[26,27] Using this criterion, the conversion of PS necessary to reach this minimum threshold can be estimated using a group contribution method[24,28] to provide a rough estimate of the surface energy of the constituent polymers, PS and poly(phenyl acetylene). In this system only 0.02% of backbone alkane bonds would need to undergo dehydrogenation to reach a Marangoni number of 80 for the smallest line and space pattern photomask used in this study (see Supporting Information for details). As previously discussed, the typical conversion in this system by FTIR is 6.4%, orders of magnitude higher than required to exceed this critical value.

Another consideration in this system is the molecular weight, M, of the polymer. Low molecular weight polymers have two clear advantages in Marangoni-driven topography formation. First, the Rouse model[29] predicts that the Marangoni number for polymer melts is independent of M in unentangled polymers (i.e., D scales as $1/\mu$). Interestingly, for entangled polymers, more common in many commercial applications, the Marangoni number theoretically decreases with increasing molecular weight, Ma ~ $M^{-1.1}$ (i.e., $\mu D \sim M^{1.1}$).[30] Therefore, higher extents of dehydrogenation are required to compensate for the M dependence of the Marangoni number for Marangoni-driven flow to occur in entangled polymers. Second, the viscosity of PS at any given temperature decreases with decreasing molecular weight which leads to the topography developing more quickly in a low viscosity film. The critical Marangoni number criterion only determines whether or not surface instabilities *will* occur but does not address the kinetics of feature formation. Therefore, to develop the pattern in the shortest time with the highest possible Marangoni number, a low M polymer is preferable such as the 2900 g/mol PS (T_g = 61 °C) that was used in this study. Another interesting feature of this process is that upon significant additional heating of the film above its T_g, on the order of hours, the features dissipate resulting in a featureless, flat film. Marangoni flow in liquids driven by reversible photochemical reactions in Newtonian liquids has previously been examined from a theoretical standpoint.[31,32] While the photochemical reaction of PS is in principle irreversible, these studies describe an interesting theoretical framework for consideration in future experiments.

To further explore the capabilities of forming line and space patterns with this method, photomasks with periods of 100 μm (Figure 3a), 25 μm (Figure 3b), and 10 μm (Figure 3c) were examined. The periodicity of features formed matches that of the photomask, while the topography exhibits curvature not present in the mask itself. Additionally, these features appear over an area as large as the output of the light source, which in principle is scalable to high-throughput processing methods. The topographical features generated in this work can be transferred into typical soft lithography mask materials like Sylgard 184,[10,33] which offers an additional avenue to pattern replication which we demonstrated in several proof of principle studies. Finally, given the photochemical conversion we observe, submicrometer features should be possible using photochemically directed Marangoni patterning.

We have also been able to easily control whether isolated features rise up from the film surface by exposure to patterned light (e.g., Figure 4a) or form depressions in the film by patterned blocking of light (e.g., Figure 4b). A sample video of

dx.doi.org/10.1021/mz300400p | *ACS Macro Lett.* 2012, 1, 1150−1154

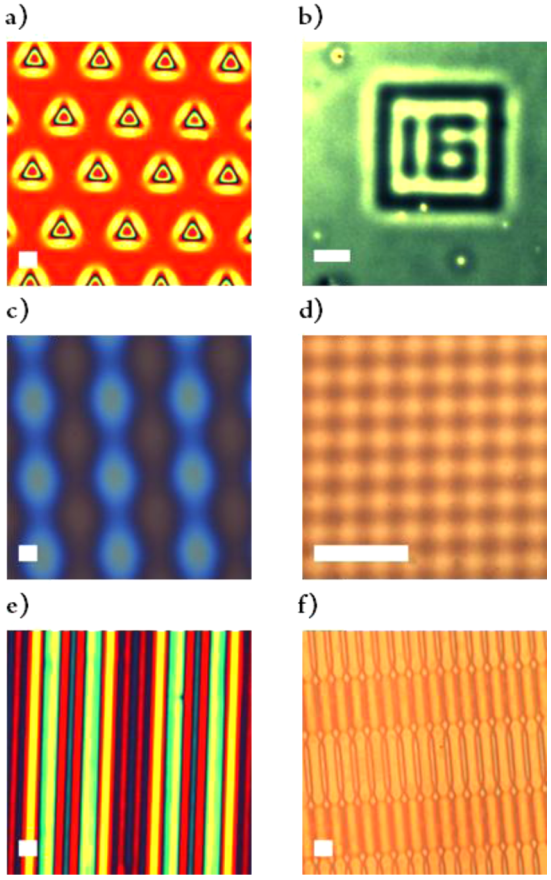

Figure 4. Various patterns formed by photochemically directed Marangoni flow. Patterns shown in (a) triagonal pillars with triangular area exposed to light, that rise up above the film, and (b) number patterns which sink into the film; both are 1:1 replications of patterns on the photomask. Patterned (c) large (formed by the 12.5 μm chrome lines on a 25 μm pitch photomask) and (d) small (formed by the 5 μm lines on a 10 μm pitch photomask) mounds are formed by exposure through the same line-and-space mask twice with the mask turned 90° between exposures. Pattern (e) lines-in-lines is the result of two exposures of different line-and-space periods parallel to each other and (f) "dogbones" by the same method with the second mask turned 90° between exposures. For (e) and (f) one exposure utilized 12.5 μm chrome lines on a 25 μm pitch photomask, while the second exposure used a 5 μm line on a 10 μm pitch photomask. Colors are interference patterns caused by changes in film height. See Supporting Information (Figure S7) for profilometery traces of parts (a) and (b) showing directionality. All films are 100–300 nm thick before patterning and have scale bars of 30 μm.

feature formation can be found in the Supporting Information where it is clear that topography forms in a matter of minutes. It is evident from this video that one way to tune the aspect ratio of the features is simply to adjust the amount of time the polymer film is heated above its T_g during topography formation. The maximum limit in aspect ratio is unclear at this point.

Formation of surface topography through directing the Marangoni Effect is not limited to lines and spaces; it can be applied to any arbitrary design as long as a UV transparent photomask is available. In this way, it is possible to transfer more complex patterns such as triangles (Figure 4a) or numbers (Figure 4b). Additionally, multiple exposures with either the same (Figure 4c,d) or different (Figure 4e,f) line-and-space masks can be used to create more complex patterns. As a point of comparison, several noncontact approaches have been previously developed for creation of topographic features in polymer films. There are methods that employ electric fields[34−39] or thermal gradients[40,41] applied to liquid polymers or monomers, sometimes with a mask in an effort to direct the resulting flow into a prescribed pattern. A recent paper showed that continuous light exposure of liquid-state PS through a close proximity photomask could also induce surface relief structures due to differences in "diffusibilities", although the light doses were also high enough to induce large molecular weight changes in the polymer.[42] It is also worth noting that there is some similarity between the features formed by the process described here and those formed by mechanical buckling instabilities,[43] growth of wrinkling patterns,[44] self-wrinkling,[45] or cross-linking directed swelling.[46] However, the mechanism of Marangoni-driven flow is substantially different, instead relying solely on gradients in surface energy induced by directed photochemical reactions of un-cross-linked polymer.

Photochemically directed Marangoni-driven flow demonstrated here originates from surface energy patterns caused by localized photochemical reactions which occur rapidly in some polymers upon exposure to light without changes in the molecular weight distribution. The topography, preprogrammed in the solid polymer by the patterned photochemical reaction, is then developed by heating to the liquid state in the absence of a mask. By contrast, many previous techniques require close proximity to a mask during formation of the desired pattern. The requirement of a close proximity mask during pattern development, rather than only during a brief exposure step, could limit the throughput of these techniques. In addition, thermal development of the pattern is fundamentally different from photoresists used in photolithography that require combinations of wet and dry postexposure processing to reveal the pattern.

In summary, this study demonstrates a new approach to creating three-dimensional topography through the photochemical generation of surface energy patterns in PS films. Dehydrogenation of the PS backbone alkane bonds by UV light results in an increase in the surface energy only in the exposed regions. Upon heating the polymer to a liquid, the Marangoni Effect causes these preprogrammed high surface energy exposed regions to rise, revealing the topography without the presence of the mask or a wet- or dry-etch development process. This process is not fundamentally limited to PS, and experiments performed using poly(para-trimethylsilylstyrene) were equally amenable. In general, this approach could be applied to any light-absorbing polymer that undergoes a photochemical change along with related formation of surface energy gradients. The short exposure and annealing times coupled with the diversity of prescribed patterns that can be created make this approach potentially useful for high-throughput processing for a wide variety of applications.

■ ASSOCIATED CONTENT

Supporting Information

Experimental procedures (including synthesis of small molecules and polymers, sample preparation, and topography development), along with the estimation of the Marangoni number, control experiments, FTIR spectra, contact angle measurements, feature profilometery, and a movie of topography formation are included. This material is available free of charge via the Internet at http://pubs.acs.org.

dx.doi.org/10.1021/mz300400p | *ACS Macro Lett.* 2012, 1, 1150−1154

AUTHOR INFORMATION

Corresponding Author

*E-mail: ellison@che.utexas.edu.

Notes

The authors declare no competing financial interest.

ACKNOWLEDGMENTS

We thank Dr. H. Celio of the UT-Austin Center for Nano- and Molecular Science and Technology for his assistance with XPS measurements, R. Deschner and Dr. C.G. Willson for providing the Photronics, Inc. photomasks, and P. Gonzales-Garza for assistance with video editing. We also thank the National Science Foundation (Grant No. 0618242) for funding the Kratos Axis Ultra XPS used in this work and the National Science Foundation CAREER Award (Grant no. DMR-1053293) for funding to all authors as well as partial financial support from the Welch Foundation (Grant No. F-1709).

REFERENCES

(1) Larson, R. G. *Angew. Chem., Int. Ed.* **2012**, *51*, 2546−2548.
(2) Scriven, L. E.; Sternling, C. V. *Nature* **1960**, *187*, 186−188.
(3) Bron, A. J.; Tiffany, J. M.; Gouveia, S. M.; Yokoi, N.; Voon, L. W. *Exp. Eye Res.* **2004**, *78*, 347−360.
(4) Cazabat, A. M.; Heslot, F.; Troian, S. M.; Carles, P. *Nature* **1990**, *346*, 824−826.
(5) Gallardo, B. S.; Gupta, V. K.; Eagerton, F. D.; Jong, L. I.; Craig, V. S.; Shah, R. R.; Abbott, N. L. *Science* **1999**, *283*, 57−60.
(6) Grunze, M. *Science* **1999**, *283*, 41−42.
(7) Strawhecker, K. E.; Kumar, S. K.; Douglas, J. F.; Karim, A. *Macromolecules* **2001**, *34*, 4669−4672.
(8) Cai, Y.; Newby, B. M. Z. *J. Am. Chem. Soc.* **2008**, *130*, 6076−6077.
(9) Wong, S.; Kitaev, V.; Ozin, G. A. *J. Am. Chem. Soc.* **2003**, *125*, 15589−15598.
(10) Xia, Y. N.; Whitesides, G. M. *Annu. Rev. Mater. Sci.* **1998**, *28*, 153−184.
(11) Briseno, A. L.; Mannsfeld, S. C. B.; Ling, M. M.; Liu, S. H.; Tseng, R. J.; Reese, C.; Roberts, M. E.; Yang, Y.; Wudl, F.; Bao, Z. *Nature* **2006**, *444*, 913−917.
(12) Wu, H. K.; Odom, T. W.; Chiu, D. T.; Whitesides, G. M. *J. Am. Chem. Soc.* **2003**, *125*, 554−559.
(13) Rolland, J. P.; Maynor, B. W.; Euliss, L. E.; Exner, A. E.; Denison, G. M.; DeSimone, J. M. *J. Am. Chem. Soc.* **2005**, *127*, 10096−10100.
(14) Rajnicek, A. M.; Britland, S.; McCaig, C. D. *J. Cell Sci.* **1997**, *110*, 2905−2913.
(15) Carman, M. L.; Estes, T. G.; Feinberg, A. W.; Schumacher, J. F.; Wilkerson, W.; Wilson, L. H.; Callow, M. E.; Callow, J. A.; Brennan, A. B. *Biofouling* **2006**, *22*, 11−21.
(16) Schumacher, J. F.; Carman, M. L.; Estes, T. G.; Feinberg, A. W.; Wilson, L. H.; Callow, M. E.; Callow, J. A.; Finlay, J. A.; Brennan, A. B. *Biofouling* **2007**, *23*, 55−62.
(17) Millan, M. D.; Locklin, J.; Fulghum, T.; Baba, A.; Advincula, R. C. *Polymer* **2005**, *46*, 5556−5568.
(18) Nagai, N.; Matsunobe, T.; Imai, T. *Polym. Degrad. Stab.* **2005**, *88*, 224−233.
(19) Nurmukhametov, R. N.; Volkova, L. V.; Kabanov, S. P. *J. Appl. Spectrosc.* **2006**, *73*, 55−60.
(20) Simons, J. K.; Chen, J. M.; Taylor, J. W.; Rosenberg, R. A. *Macromolecules* **1993**, *26*, 3262−3266.
(21) Zhang, D.; Dougal, S. M.; Yeganeh, M. S. *Langmuir* **2000**, *16*, 4528−4532.
(22) Mundra, M. K.; Ellison, C. J.; Behling, R. E.; Torkelson, J. M. *Polymer* **2006**, *47*, 7747−7759.
(23) Coates, J. In *Encyclopedia of Analytical Chemistry*; Meyers, R. A., Ed.; John Wiley & Sons Ltd.: Chichester, 2000; pp 10815−10837.
(24) *Polymer Handbook*; Brandrup, J., Immergut, E. H., Grulke, E. A., Eds.; Wiley and Sons: Hoboken, NJ, 1999.
(25) Wu, K. H.; Lu, S. Y.; Chen, H. L. *Langmuir* **2006**, *22*, 8029−8035.
(26) Reichenbach, J.; Linde, H. *J. Colloid Interface Sci.* **1981**, *84*, 433−443.
(27) Weh, L. *Mater. Sci. Eng. C: Biomimetic Supramol. Syst.* **1999**, *8−9*, 463−467.
(28) Bicerano, J. *Prediction of Polymer Properties*, 3rd ed.; Marcel Dekker, Inc.: New York, 2002.
(29) Doi, M.; Edwards, S. F. *The Theory of Polymer Dynamics*; Clarendon Press: Oxford, 1986.
(30) Hiemenz, P.; Lodge, T. P. *Polymer Chemistry*, 2nd ed.; CRC Press: Boca Raton, FL, 2007.
(31) Golovin, A. A.; Volpert, V. A. *Phys. Fluids* **2007**, *19*, 122104.
(32) Golovin, A. A.; Volpert, V. A. *Math. Model. Nat. Phenom.* **2008**, *3*, 27−54.
(33) Qin, D.; Xia, Y. N.; Whitesides, G. M. *Nat. Protoc.* **2010**, *5*, 491−502.
(34) Dickey, M. D.; Collister, E.; Raines, A.; Tsiartas, P.; Holcombe, T.; Sreenivasan, S. V.; Bonnecaze, R. T.; Willson, C. G. *Chem. Mater.* **2006**, *18*, 2043−2049.
(35) Dickey, M. D.; Raines, A.; Collister, E.; Bonnecaze, R. T.; Sreenivasan, S. V.; Willson, C. G. *J. Mater. Sci.* **2008**, *43*, 117−122.
(36) Morariu, M. D.; Voicu, N. E.; Schaffer, E.; Lin, Z. Q.; Russell, T. P.; Steiner, U. *Nat. Mater.* **2003**, *2*, 48−52.
(37) Schaffer, E.; Thurn-Albrecht, T.; Russell, T. P.; Steiner, U. *Nature* **2000**, *403*, 874−877.
(38) Wu, N.; Russel, W. B. *Appl. Phys. Lett.* **2005**, *86*, 241912.
(39) Wu, N.; Russel, W. B. *Nano Today* **2009**, *4*, 180−192.
(40) Chou, S. Y.; Zhuang, L. *J. Vac. Sci. Technol. B* **1999**, *17*, 3197−3202.
(41) Chou, S. Y.; Zhuang, L.; Guo, L. *J. Appl. Phys. Lett.* **1999**, *75*, 1004−1006.
(42) Ubukata, T.; Moriya, Y.; Yokoyama, Y. *Polym. J.* **2012**, *44*, 966−972.
(43) Chiche, A.; Stafford, C. M.; Cabral, J. T. *Soft Matter* **2008**, *4*, 2360−2364.
(44) Chung, J. Y.; Nolte, A. J.; Stafford, C. M. *Adv. Mater.* **2009**, *21*, 1358−1362.
(45) Chandra, D.; Crosby, A. J. *Adv. Mater.* **2011**, *23*, 3441−3445.
(46) Kim, J.; Hanna, J. A.; Byun, M.; Santangelo, C. D.; Hayward, R. C. *Science* **2012**, *335*, 1201−1205.